Environment International 147 (2021) 106359

Contents lists available at ScienceDirect

Environment International

journal homepage: www.elsevier.com/locate/envint

Coastal vulnerability to climate change in China's Bohai Economic Rim

Yan Zhang [a], Tong Wu [a], Katie K. Arkema [b,c], Baolong Han [a], Fei Lu [a], Mary Ruckelshaus [b,c], Zhiyun Ouyang [a,*]

[a] State Key Laboratory of Urban and Regional Ecology, Research Center for Eco-Environmental Sciences, Chinese Academy of Sciences, Beijing 100085, China
[b] The Natural Capital Project, Stanford University, Stanford, CA 94305-5020, United States
[c] School of Environmental and Forest Sciences, University of Washington, Seattle, WA 98195, United States

ARTICLE INFO

Handling Editor: Hefa Cheng

Keywords:
Climate change
Vulnerability assessment
Sea level rise
Coastal zone management
InVEST

ABSTRACT

Climate change and human activities exert a wide range of stressors on urban coastal areas. Synthetical assessment of coastal vulnerability is crucial for effective interventions and long-term planning. However, there have been few studies based on integrative analyses of ecological and physical characteristics and socioeconomic conditions in urban coastal areas. This study developed a holistic framework for assessing coastal vulnerability from three dimensions - biophysical exposure, sensitivity and adaptive capacity - and applied it to the coast of Bohai Economic Rim, an extensive and important development zone in China. A composite vulnerability index (CVI) was developed for every 1 km^2 segment of the total 5627 km coastline and the areas that most prone to coastal hazards were identified by mapping the distribution patterns of the CVIs in the present and under future climate change scenarios. The CVIs show a spatial heterogeneity, with higher values concentrated along the southwestern and northeastern coasts and lower values concentrated along the southern coasts. Currently, 20% of the coastlines with approximately 350,000 people are highly vulnerable to coastal hazards. With sea-level rises under the future scenarios of the year 2100, more coastlines will be highly vulnerable, and the amount of highly-threatened population was estimated to increase by 13–24%. Among the coastal cities, Dongying was categorized as having the highest vulnerability, mainly due to poor transportation and medical services and low GDP per capita, which contribute to low adaptive capacity. Our results can benefit decision-makers by highlighting prioritized areas and identifying the most important determinants of priority, facilitating location-specific interventions for climate-change adaptation and sustainable coastal management.

1. Introduction

Coastal areas cover less than 10% of global terrestrial surface but sustain one-third of the world's population (UNEP, 2006). These areas have been experiencing a wide range of stressors from both climate change and human activities (Gabler et al., 2017; IPCC, 2014; Sekovskia et al., 2012), which threaten human lives and properties. Coastal habitats play an important role in mitigating the impacts of natural hazards and provide a broad range of collateral benefits to human well-being (e.g., foodstuffs and habitat provision, wastewater treatment, recreational opportunities) (Arkema et al., 2013). However, global sea level rise and coastal flooding are expected to increase significantly by mid-century (Hansen et al., 2016), while rapid urbanization with intensive human activities may accelerate the degradation of coastal ecosystems (Sekovskia et al., 2012). Together these factors are likely to increase coastal vulnerability to natural hazards and put coastal populations and properties in harms' way.

Vulnerability refers to the degree to which a system is susceptible to natural hazards and social changes (Bevacqua et al., 2018; Sahin and Mohamed, 2014). Numerous studies have been conducted worldwide to examine different aspects of coastal vulnerability. For instance, Onat et al. (2018) estimated the exposure characteristics of Hawai'i's coastlines by considering seven biophysical factors. Some studies focused on socioeconomic factors crucial to building resilience to climate change threats (Kantamaneni et al., 2018; Serafim et al., 2019; Yadav and Barve, 2017; Zhu et al., 2019). Overall, vulnerability comprises a set of conditions and processes resulting from both environmental and socioeconomic factors that increase the susceptibility of coastal communities to natural hazards, and can also encompass the notion of coping capacity to respond to their impacts (Hahn et al., 2009; IPCC, 2014). Although studies assessing the overall vulnerability of China's coasts exist (Lu et al., 2014; Sajjad et al., 2018; Wang et al., 2014), they have mainly

* Corresponding author.
E-mail address: zyouyang@rcees.ac.cn (Z. Ouyang).

https://doi.org/10.1016/j.envint.2020.106359
Received 8 October 2020; Received in revised form 5 December 2020; Accepted 18 December 2020
Available online 30 December 2020

focused on geomorphologic and physical dimensions. To date, synthetical assessments of the vulnerability status based on an integration of biophysical exposure, sensitivity and adaptive capacity of coastal communities are not well understood.

A variety of methods have been used to assess coastal vulnerability by incorporating different factors that indicate different dimensions (Arkema et al., 2013; Bevacqua et al., 2018; Hinkel and Klein, 2009). Inclusion of different factors into an assessment framework relies largely upon data availability and the context of different studies. Modeling spatial vulnerability at a fine scale based on an integration of representative factors is helpful in identifying the most vulnerable areas for prioritized interventions. Ecosystem service models like the Integrated Valuation of Ecosystem Services and Tradeoffs (InVEST) show the impacts of changes in ecosystems and associated services at different spatial scales, and have been widely used to understand the biophysical vulnerability of coastlines globally (Arkema et al., 2013; Hopper and Meixler, 2016; Onat et al., 2018; Sajjad et al., 2018). To date, few models integrate ecological, physical and socioeconomic factors into synthetical vulnerability assessments of coastal areas. In this study, such an integrated analysis was conducted for the Bohai Economic Rim (BER), an extensive and important development zone with rapid population growth and intensified human activities in China.

The BER stretching along three provinces and one provincial-level municipality has experienced frequent storms and typhoons, and will be increasingly exposed to climate change impacts in the decades ahead (Wang et al., 2018). According to the China Sea Level Bulletin (SOA, 2017), the relative sea level of Bohai owing to climate change was predicted to rise by over 50 mm in the next 30 years, placing coastal communities at greater risks. As an important economic development zone in China, this region covers 5% of land area, but accounts for 18% of its total population and contributes to 25% of national GDP (Gao et al., 2014). The BER's rapid socioeconomic development has exacerbated ecological problems, such as wetland loss, coastal erosion and water quality deterioration (Gao et al., 2014; Lu et al., 2014), thereby reducing the resilience of coastal communities to natural hazards. Since the introduction of the Belt and Road Initiative development strategy in 2013, a series of new investment and trade projects have been steadily adopted and the coastal economic growth has intensified (Oliveira et al., 2020). In response, sustainable coastal development has attracted significant attention from the central and local governments. A synthetical vulnerability assessment that can aid in the identification of hazard-prone areas and the preparation of location-specific interventions is needed to facilitate the sustainable development.

To bridge the knowledge gap, this study was undertaken with the following objectives: 1) to develop a holistic framework for synthetic vulnerability assessments by integrating ecological, physical and socioeconomic factors into a spatial representation at a segment scale; 2) to identify areas most vulnerable to sea-level rises and storm surges; and 3) to identify critical factors that affect the condition of coastal vulnerability.

2. Methods

2.1. Study area

The BER is composed of three provinces (Liaoning, Hebei, Shandong) and one municipal city (Tianjin) (Fig. 1). Several major rivers including the Liao, Luan, Hai and Yellow Rivers flow through this region to the Bohai Sea, which is semi-enclosed by three bays - Liaodong Bay, Bohai Bay and Laizhou Bay. In this study, the coastal areas assessed has a total coastline of 5627 km in length and a diverse physical characteristic. Over 80% of the coastline is composed of artificial coasts, such as revetment and rip-rap wall, whereas the remaining coastline is composed of natural coasts, such as rock cliff, rock platform, alluvial

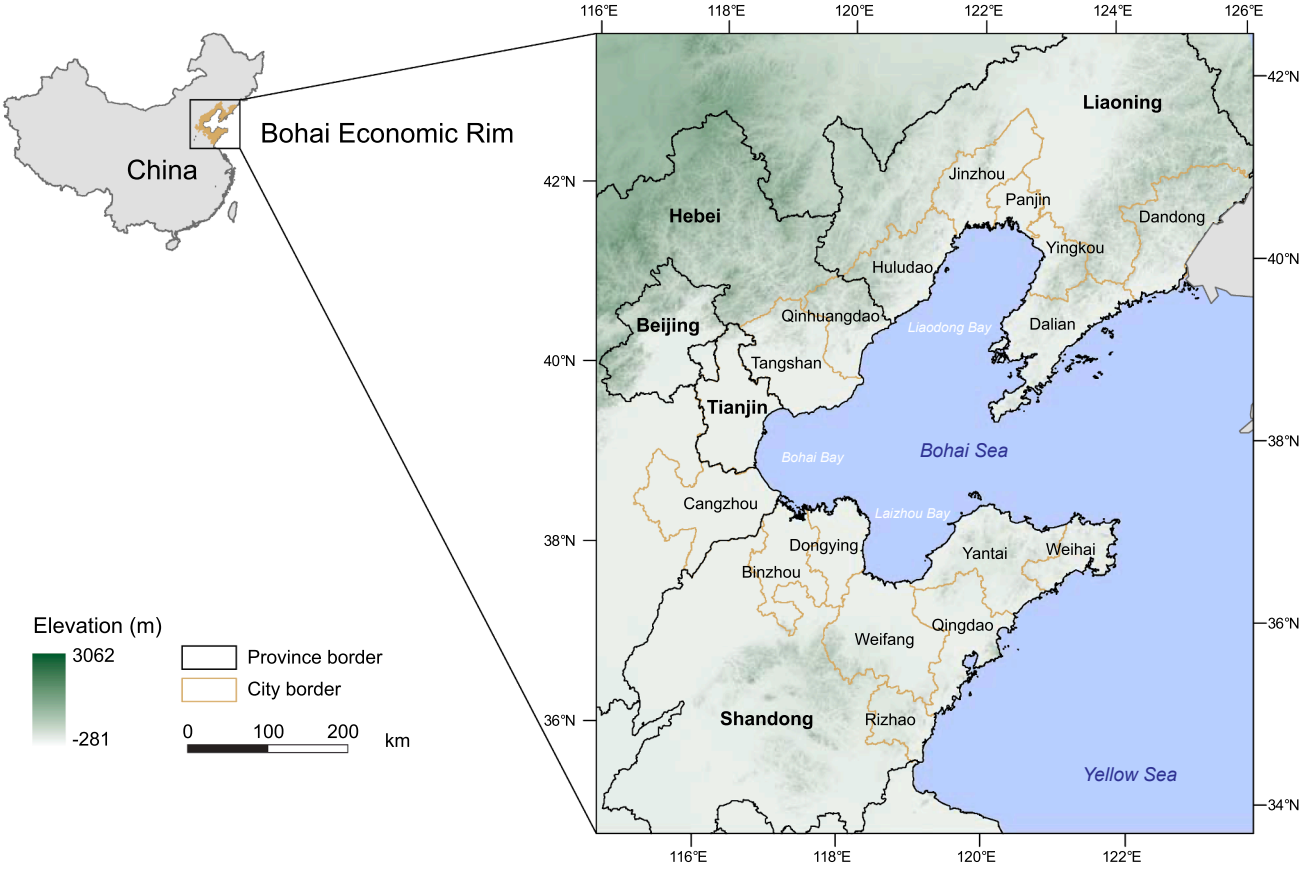

Fig. 1. Location of the Bohai Economic Rim.

plain, gravel beach, estuary, sand beach and mud flat (Wei et al., 2019). This region is characterized by a temperate semi-humid monsoon climate with a 10-year-averaged annual temperature of 11.2 °C and an annual average precipitation of 687.5 mm (Gao et al., 2014). The hot summer weather is often followed by heavy rainfall, frequent thunderstorms and typhoons, which cause frequent inundation events, especially in low-lying areas. Under the coupling influence of geological and climatic factors, the BER has a diversity in the spatial pattern of main coastal hazards, with storm surges for the Liaodong Bay and Bohai Bay, and seawater intrusion and soil erosion for the Laizhou Bay (Liu et al., 2017). According to the Bulletin of China Marine Disaster (MNR, 2020), a total of 69 storms was recorded during 2010–2019, which caused an economic loss of 10.4 billion CNY, accounting for over 50% of total economic losses due to coastal hazards.

As an important economic center in China and the northeast Asia (Liu et al., 2017), the BER has experienced rapid urbanization and economic development over recent years. The successful implementation of China's Important Economic Zones and Port Group policy since the beginning of the 21st century has led to an intensive expansion of urbanized areas with rapid population aggregation in this region. According to the National Bureau of Statistics (NBS, 2020), the total gross domestic product (GDP) of the BER accounted for approximately 14.7% of the total value for China in 2019, with almost 3 times higher for Shandong compared to that for Liaoning and Hebei provinces.

Nonetheless, the development prospect of the BER is being threatened by the degradation and loss of ecosystems. The corresponding loss of ecosystem services, exacerbated by the worsening influence of climate change, have increased the frequency and intensity of coastal hazards. Recent events including the flooding caused by the storms of Mojie and Anbi in 2018 and Liqima in 2019, which devastated the BER and caused a total economic loss of 3.0 billion CNY (MNR, 2020), demonstrate the urgent need for a deeper and more comprehensive understanding of the coastal vulnerability to inform planning for climate change adaptation.

2.2. Overview of the vulnerability index

The conceptual structure of the vulnerability index based on an analytical hierarchy process was shown in Fig. 2. In this study, the composite vulnerability index (CVI) refers to the extent to which coastal systems are susceptible to the impacts of sea level rise and storm surges. The CVI was determined as a function of exposure index (EI), sensitivity index (SI) and adaptive capacity index (ACI). The EI and SI refer to the propensity of coastal populations and properties to be adversely affected by natural hazards (Arkema et al., 2013), whereas the ACI refers to the ability of coastal communities to reduce the impacts of natural hazards (Hahn et al., 2009). Totally, the entire coastline was divided into 5627 segments, with a resolution of 1 km × 1 km for each segment. Following the establishment of the index system, index values were assigned to each coastal segment.

2.3. Exposure index (EI)

The EI was calculated using the coastal vulnerability model in InVEST, an open-source tool developed by the Natural Capital Project (https://naturalcapitalproject.stanford.edu/). The model, which is built on previous analytical approaches (Arkema et al., 2013; Gornitz, 1990; Hammar-Klose and Thieler, 2001), quantifies the impacts of sea level rise and storm surges on biophysical exposure by incorporating seven factors: geomorphology, relief, habitat, sea level rise, wind, wave and surge potential. According to the criteria described by Sharp et al. (2016) and Arkema et al. (2013), the inputs were ranked from 1 (very low) to 5 (very high) for different exposure levels (Supplementary Table S1), after which the EI for each segment was calculated as:

$$\text{Index} = \left(\prod_{i=1}^{n} R_n\right)^{1/n} \quad (1)$$

where Index refers to the EI (or other vulnerability indices such as SI and ACI). R_n is the rank of the factors for each vulnerability index and n is the number of factors.

The geomorphologic characteristic refers to the resistance of coastal areas against inundation and erosion. Based on the classification criteria in the InVEST User's Guide, a polyline layer with nine geomorphology classes including rock cliff, rock platform, revetment, rip-rap wall, alluvial plain, gravel beach, estuary, sand beach and mud flat, was created in the Google Earth Image 2018. The created polylines were modified based on field investigations along the coast and an exposure rank was assigned to each segment. Coastal defense structures were included in the geomorphology layer, and were assigned as a moderate exposure level (R = 3) as they could fail in preventing inundation from extreme events (Sharp et al., 2016).

The digital elevation model with a spatial resolution of 30 m, provided on the Geospatial Data Cloud (http://www.gscloud.cn/), was used to generate an elevation rank for each segment (GIMCP, 2018), and the average elevation within a radius of 3 km was determined to approximate the variation in coastal relief.

The habitat layers were generated using data from a wide range of sources (Chen et al., 2014; Mcowen et al., 2017; UNEP-WCMC, 2018). Four types of coastal habitats (coastal forest, grassland, saltmarsh and intertidal aquatic vegetation) were included in the model

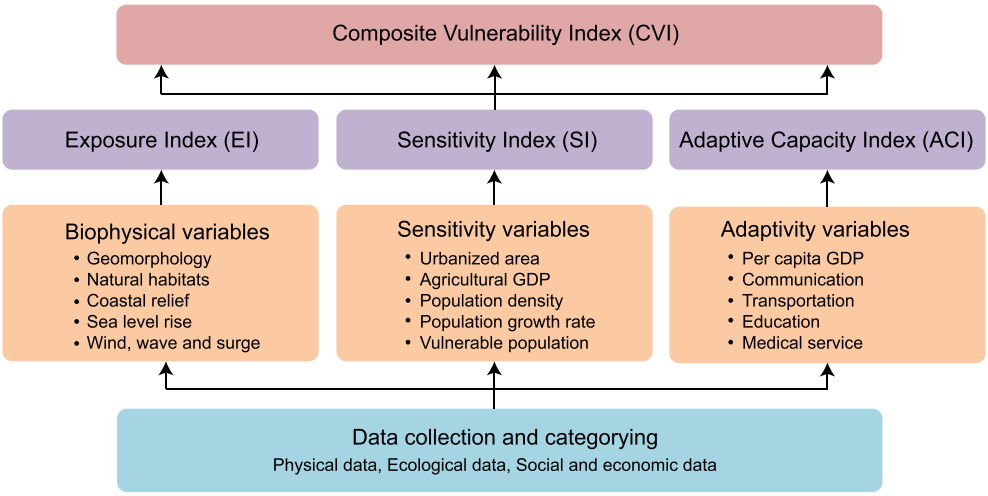

Fig. 2. Hierarchy process for the composite vulnerability in the Bohai Economic Rim.

(Supplementary Fig. S1). The model then calculated whether each segment benefited from reduced exposure provided by the ecosystems based on the distance from each segment to each grid cell of habitat and the protective distance of each habitat (Supplementary Table S2). If no habitats were found in the calculation, an exposure rank of 5 was assigned to the segment. For a segment protected by more than one habitat type, the combined effects were calculated based on their separate exposure ranks (Sharp et al., 2016):

$$R_{Hab} = 4.8 - 0.5\sqrt{\left(1.5\max_{i=1}(5 - R_i)\right)^2 + \sum_{i=1}^{N}(5 - R_i)^2 - \left(\max_{i=1}(5 - R_i)\right)^2} \quad (2)$$

where R_{Hab} is the overall rank of habitats and N is the number of habitat types.

Current sea-level changes were calculated as the increase in water elevation from 1992 to 2018 using the tidal gauge data from the Permanent Service for Mean Sea Level (PSMSL, 2018). To access the variability of coastal vulnerability in the context of changing climate, sea level projections with a probability of 95% along the BER coast were estimated for 2100 under the RCP 4.5 and RCP 8.5 scenarios from the fifth phase of the Coupled Model Intercomparison Project (CMIP5) model according to the study of Qu et al. (2019), which considered the impacts of glacial isostatic adjustment and local land-motion, steric and mass redistribution due to mass fluxes from glaciers, ice sheets and land–water storage changes. RCP 4.5 represents a stabilization scenario with moderate sea level rises, while RCP 8.5 represents the worst-possible-case with the highest sea level rises by the end of this century (Supplementary Fig. S2).

To calculate the surge potential, a fetch distance was determined by measuring the distance between the segment and the edge of the continental shelf (NCP, 2018). The threshold for distinguishing exposed coastlines from sheltered coastlines was considered as the average distance within inshore fjords. For the wind and wave exposure factors, the highest 10% wind speed in each of 16 equiangular sectors were extracted from a compiled eight-year (2008–2016) of WAVEWATCH III model dataset (NCP, 2018). The relative exposure to wind and waves were calculated as follows (Sharp et al., 2016):

$$E_{wind} = \sum_{i=1}^{16} U_i P_i F_i \quad (3)$$

$$E_{wave} = \max(E_w^o, E_w^l) \quad (4)$$

$$E_w^o = \sum_{i=1}^{16} H[F_i] P_i^o O_i^o \quad (5)$$

$$E_w^l = \sum_{i=1}^{16} P_i^l O_i^l \quad (6)$$

where E_{wind} is the wind exposure ($m^2\ s^{-1}$); U_{i} is the average of the highest 10% wind speed ($m\ s^{-1}$); P_{i} is the percentage of wind blowing in the i-th sector within all wind speed in the record of interest; F_{i} is the fetch distance (m); E_{wave} is the wave exposure ($kW\ m^{-1}$); E_w^o and E_w^l are oceanic and locally wind-generated wave power, respectively ($kW\ m^{-1}$); $H[F_{\mathrm{i}}]$ is a Heaviside step function of fetch distance; P_i^o and P_i^l are the averages of the highest 10% power for respective wave types ($kW\ m^{-1}$); O_i^o and O_i^l are the wave duration for respective wave types (s); i is the wind sector.

2.4. Sensitivity index (SI)

The sensitivity and adaptive capacity factors were collected based on an extensive review of previous studies and expert judgement. Specific sources for the sensitivity and adaptive capacity factors were listed in Supplementary Table S3. In this study, the SI was calculated as an aggregation of five factors - urbanized area, agricultural GDP, population density, population growth rate and vulnerable population - using Eq. (1). The urbanized area within the limit of each segment was assigned to the coastal segment, while city-level datasets were used for the population growth rate factor. For the vulnerable population factor, we quantified the combined effects of people over 65-years old, the illiterate population and families below the poverty line. The proportions of these three demographic factors in relation to the total population were calculated and the scores of the first component were extracted using principle component analysis.

2.5. Adaptive capacity index (ACI)

The ACI was calculated as an aggregation of five factors - communication, education, per capita GDP, transportation and medical services - using Eq. (1). In the case of the communication, education, transportation and medical service factors, which were combined measures of different contributors (Supplementary Table S3), the scores of first principle component for each factor were extracted by incorporating the contributors into principle component analysis. In this study, we considered the proportion of the populations using mobile phone, fixed telephone and internet in relation to the total population as the contributors for communication service; the school density and the proportion of educated populations in relation to the total population for education service; the distance to nearest hospital and density of general hospital for medical service; the distance to nearest station, number of private cars, density of road and rail networks and density of bus stations and ports for transportation service. To better approximate the spatial variation in the contributors, density datasets were determined as averages with a 3-km radius from respective input layers.

2.6. Composite vulnerability index (CVI)

The CVI was calculated as positive correlation with EI and SI, but as negative correlation with ACI (Krishnan et al., 2019):

$$\mathrm{CVI} = (EI \times SI)/ACI \quad (7)$$

To better delineate the variation in vulnerability condition along the coast, the distribution of CVIs was categorized into quartiles to represent high (upper 25%), medium (central 50%) and low (lower 25%) vulnerability categories. City-level factors of biophysical exposure, sensitivity and adaptive capacity were determined by taking the median values of the model inputs assigned for the coastal segments. The city-level indices of EI, SI and ACI were determined by taking the city-level factors assigned for each dimension.

3. Results

3.1. Exposure index (EI)

The EIs ranged between 1.22 and 4.84 along the coastlines (Fig. 3a). Approximately one-third of the total segments, concentrated in the eastern and southern regions of Shandong province and the southern region of Dalian city, have low exposure scores, while the remaining segments have medium to high exposure scores. The EIs vary with a geographical heterogeneity among the coastal cities, with Cangzhou registering the highest values (Fig. 4a), which was mainly caused by relatively higher scores on wind speed and wave height factors compared to other coastal cities (Fig. 5). In contrast, Weihai has the lowest biophysical exposure, mainly attributed to lower scores on the sea level rise and coastal relief factors. At the city scale, the highly-exposed segments account for over half of the total segments for Tangshan, Cangzhou and Yingkou, and approximately one-third of the total segments for Tianjin, Dongying, Binzhou and Weifang, but <10% of the

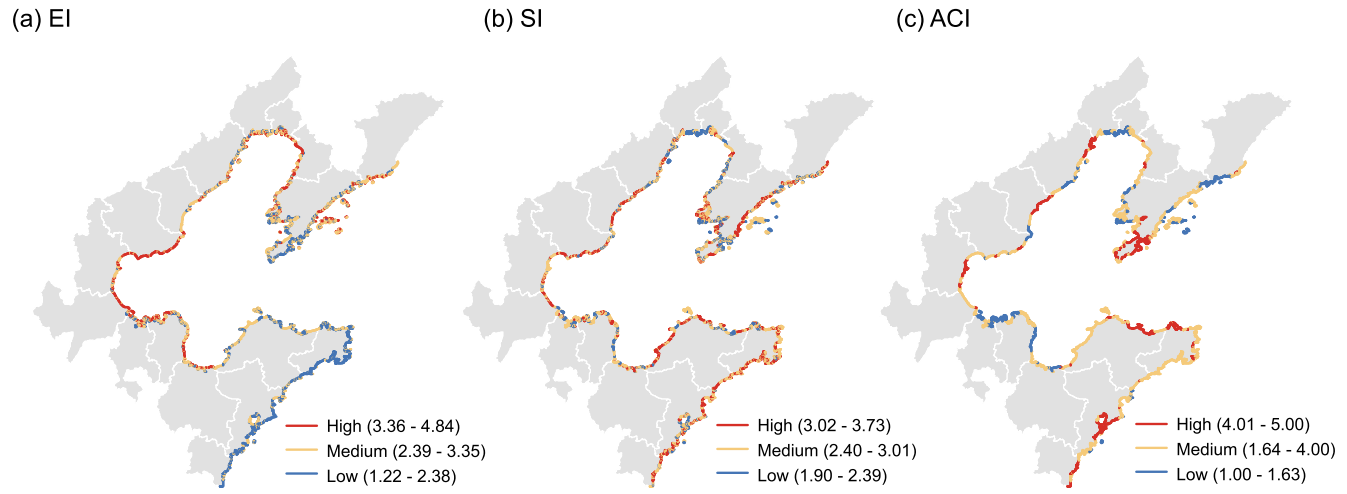

Fig. 3. Vulnerability indices (EI, Exposure Index. SI, Sensitivity Index. ACI, Adaptive Capacity Index) along the coast of the Bohai Economic Rim. Cut-offs for high (red, upper 25%), medium (yellow, centre 50%) and low (blue, lower 25%) categories of each vulnerability index are based on the distribution of index values. (For interpretation of the references to colour in this figure legend, the reader is referred to the web version of this article.)

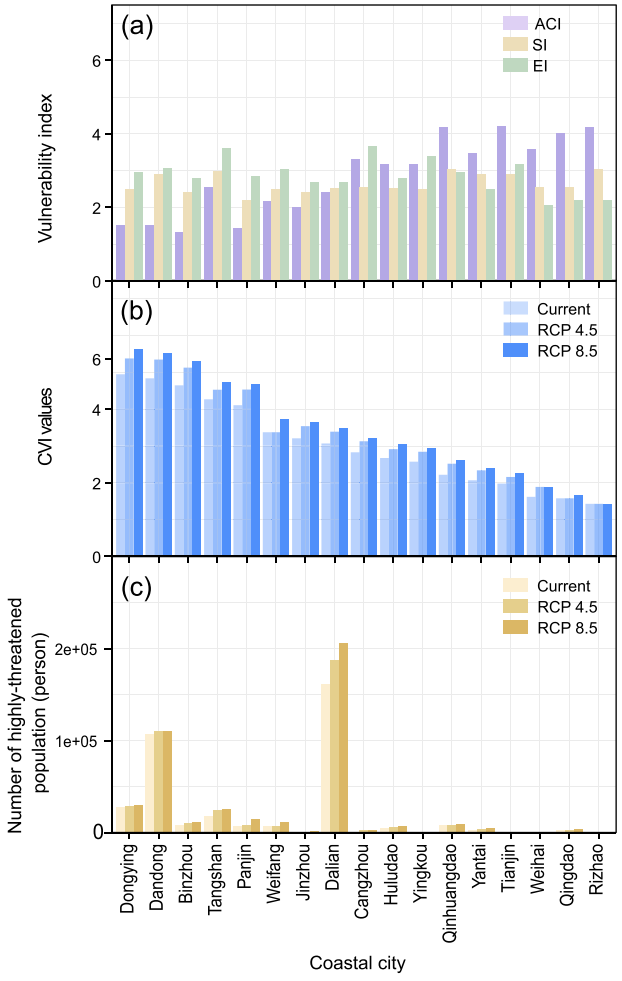

Fig. 4. Vulnerability condition for each coastal city in the Bohai Economic Rim. (a) Vulnerability indices of adaptive capacity (ACI), sensitivity (SI) and exposure (EI); (b) Composite vulnerability index (CVI); and (c) the number of highly-threatened population under current and future scenarios. RCP 4.5 and RCP 8.5 represent the Representative Concentration Pathway scenarios of 4.5 and 8.5 by 2100, respectively.

total segments for other cities.

3.2. Sensitivity index (SI)

The SIs ranged between 1.90 and 3.73 along the coastlines (Fig. 3b). Approximately one-quarter of the total segments were categorized as having either high or low scores, while the remaining segments were categorized as having medium scores. Of all the coastal cities, the SI is the highest for Rizhao (Fig. 4a), which mainly resulted from higher scores on the urbanized area factor compared to other cities (Fig. 5). In contrast, the SI is the lowest for Panjin, which mainly resulted from lower scores on the population density, population growth rate and urbanized area factors. Over half of the coastal segments in the cities of Jinzhou and Panjin have low scores, while most of the segments in other coastal cities fall in the medium to high sensitivity categories.

3.3. Adaptive capacity index (ACI)

The ACIs ranged between 1 and 5 along the coastlines (Fig. 3c). Approximately one-quarter of the total segments have either high or low adaptive capacity scores, while the remaining segments have medium adaptive capacity scores. The ACIs show a high spatial heterogeneity among the coastal cities, with the highest value found for Tianjin and the lowest value found for Binzhou (Fig. 4a). The dominating contributor to the high adaptive capacity of Tianjin was found to be better public facilities and services, such as transportation, communication, education and medical services, as well as higher per capita GDP compared to other cities (Fig. 5), while the adaptive capacity of Binzhou was mainly lowered down by relatively lower scores on these factors. Over half of the coastal segments in the cities of Tianjin, Rizhao and Qinhuangdao have high adaptive capacity scores, while less than one-third of the coastal segments with high adaptive capacity scores were found in other cities, especially in Binzhou, Dongying and Panjin, where all segments were categorized as having low to medium scores.

3.4. Composite vulnerability index (CVI)

Currently, almost twenty percent of the total segments fall in the high vulnerability category, and they are mainly distributed along the southwestern and northeastern coastlines (Fig. 6a). Coastal segments categorized as having low or medium vulnerability scores account for one-third and more than one-half of the total segments, respectively. With the rising sea levels by 2100, the overall vulnerability was

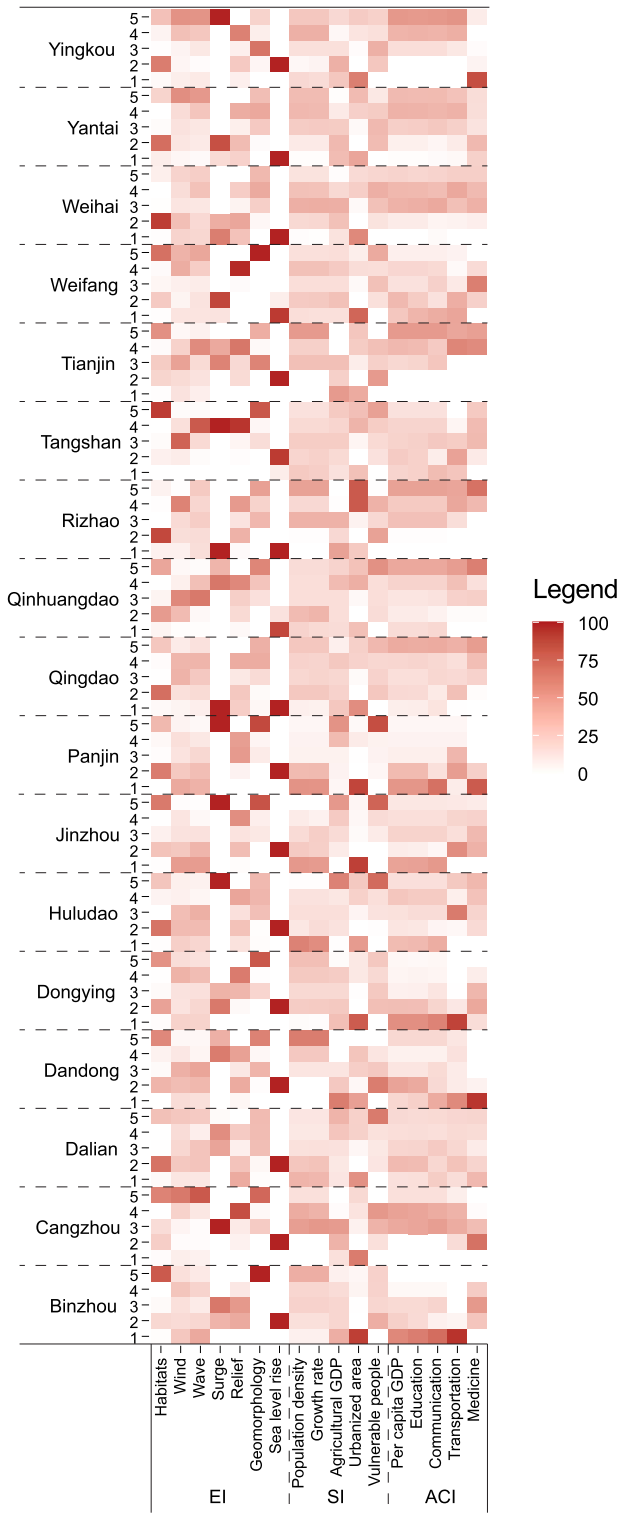

Fig. 5. Proportion of coastal segments (%) with different ranks (1–5) for the factors forming the indices of exposure (EI) sensitivity (SI) and adaptivity (ACI) for each coastal city.

projected to increase, with the number of highly-vulnerable segments increasing by 24–36%, whereas the number of low-vulnerable segments falling by 19–24%, over the current circumstances. Although there is a similarity in the spatial distribution of coastal segments with different vulnerability levels across different scenarios, major increases in the number of highly-vulnerable segments were found in the north coast of Liaodong Bay and the south coast of Bohai Bay under the RCP 4.5 and RCP 8.5 scenarios (Fig. 6b and c).

The CVIs for the coastal cities show a great spatial heterogeneity, with the values ranging from 1.43 for Rizhao to 4.95 for Dongying in the present (Fig. 4b). The CVIs are highly associated with the ACIs ($r = -0.824$, $P < 0.001$). In contrast, the positive correlations of ACIs are weak for both EIs ($r = 0.615$, $P < 0.001$) and SIs ($r = 0.601$, $P < 0.001$). Furthermore, little relationships were found among the three vulnerability indices (absolute $r = 0.109–0.354$). The highest vulnerability for Dongying is mainly associated with its relatively lower adaptive capacity coupled with higher exposure and community sensitivity compared to other cities (Fig. 4a). In contrast, the lowest vulnerability for Rizhao is associated with its relatively higher adaptive capacity coupled with lower exposure and community sensitivity, which was mainly attributed to lower scores on the sea level rise and urbanized area factors. Among the coastal cities, over half of the highly-vulnerable segments were found in Dongying, Dandong and Binzhou, whereas most of the coastal segments were categorized as having low to medium vulnerability in other coastal cities, especially in Rizhao and Tianjin, where the coastal segments only fall in low and medium vulnerability categories.

Based on the vulnerability conditions under different scenarios, coastal population that most threatened by coastal hazards were estimated. Currently, about 350,000 people, accounting for 8.9% of the total coastal population in the BER, are living in areas most prone to coastal hazards, with larger number of highly-threatened population found in Dalian and Dandong compared to other cities (Fig. 4c). With sea-level rises by 2100, the number of highly-threatened population was estimated to increase by 13–24% over the current scenario and approximately 402,000 to 440,000 people were projected to live in areas most prone to coastal hazards.

4. Discussion

Globally, rapid urbanization combined with climate change have exert great stresses on coastal areas, placing large numbers of people and ecosystems highly exposed to the threats of natural hazards (Barbier, 2014; Xu et al., 2019). This study presented a framework for synthetical vulnerability assessments by integrating ecological, physical and socioeconomic factors in to a single spatial representation of vulnerability status. To provide a comprehensive picture, we estimated the CVIs as a function of three indices (EI, SI and ACI) that indicate critical aspects of coastal vulnerability, since biophysical exposure together with sensitivity represent the probability of coastal systems to be adversely affected by natural hazards (Arkema et al., 2013; Sahin and Mohamed, 2014), whereas adaptive capacity reduces the impacts of natural hazards (Hahn et al., 2009).

The lower vulnerability of coastal cities located in the south of the BER (e.g., Rizhao, Qingdao, Weihai) are related to the lower biophysical exposure attributed to the presence of coastal natural habitats studied, which play a vital role in coastal protection by reducing the impacts of coastal storms and erosion. This is consistent with previous studies, which reported an important role of coastal ecosystems in stabilizing shorelines and reducing coastal risks for some coastal States around the world (Arkema et al., 2013; Gedan et al., 2011). Additionally, the high adaptive capacity of these cities due to their higher development levels in terms of transportation, communication, education and medical services, provide favorable socioeconomic conditions to respond to coastal hazards. In contrast, the higher vulnerability of coastal cities along the south coast (e.g., Dongying, Binzhou) and the northeast coast (e.g., Dandong), are partly due to their lower adaptive capacity, suggesting that these cities are more likely to be affected by coastal hazards compared to other cities. A similarity in the spatial pattern of these cities was also found by Wang et al. (2014), who mapped the risks of coastal cities using a Risk Matrix Approach. Among the coastal cities, the city most prone to natural hazards was found to be Dongying. The fringing habitats like coastal forests and saltmarshes provide it with nature-based

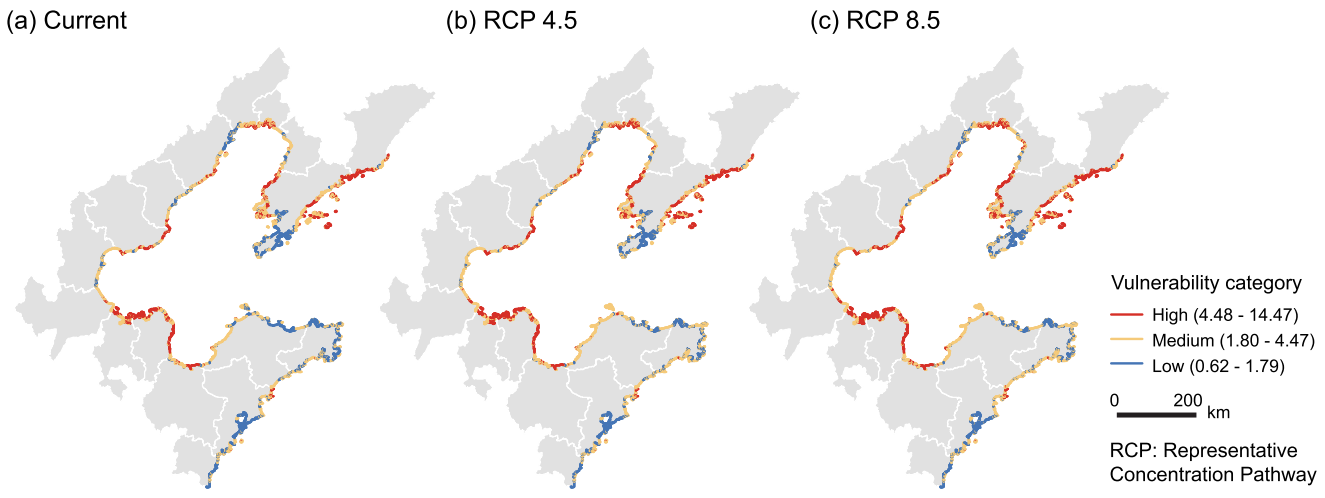

Fig. 6. Composite vulnerabilty index (CVI) under current and future (2100) scenarios (RCP4.5, RCP8.5) along the coast of the Bohai Economic Rim. Cut-offs for high (red, upper 25%), medium (yellow, centre 50%) and low (blue, lower 25%) categories are based on the distribution of index values. (For interpretation of the references to colour in this figure legend, the reader is referred to the web version of this article.)

defenses against storm surges and waves, decreasing its biophysical exposure level. However, this city suffers from underdevelopment in social matters associated with hazard adaptation, as indicated by lower scores for the per capita GDP, medical and transportation service factors. This led to lower adaptive capacity to cope with natural hazards, resulting in higher vulnerability compared to other cities. The impacts of adaptivity capacity on the overall vulnerability was also evidenced by the significant correlation of ACIs with CVIs, suggesting that adaptive capacity had influences on vulnerability status, which is in accordance with previous studies (Brooks et al., 2005; Yadav and Barve, 2017), which attempted to identify the factors driving the social-economic vulnerability of coastal cities. These results demonstrated that adaptation capacity plays an important role in assessing the composite vulnerability to climate change and should be incorporated into the assessment of, and the mitigation preparation for, coastal hazards.

Although the framework in this study offered a set of projections on the spatial and temporal patterns of coastal vulnerability, there are still limitations on its application: 1) The extent of coastal zones as well as habitat covers change over time due to various coupled natural and human-induced disturbances. However, we used the same datasets of coastlines and habitat coverage for all projected scenarios. In addition, the quality and structure of natural habitats serve an important role in coastal protection (Arkema et al., 2013; Sharp et al., 2016). However, these factors were not considered due to data deficiency; 2) Upstream human activities, such as the construction of reservoirs and other "grey" infrastructure, could trap silt and sand from moving to the coastal areas. The decreased sediment discharges and sedimentation rates could exacerbate the impacts of sea level rise by causing coast erosion and ecosystem loss (Gedan et al., 2011; Phillips et al., 2009). Other human activities that affect coastal environments, such as sewage pollution, algal blooms and oil spills, are also relevant to the vulnerability condition (Beroya-Eitner, 2016; Brooks et al., 2005; Gao et al., 2014; He and Silliman, 2019). Further studies could include factors relating to individual and interactive impacts of these bio-geophysical processes; 3) A simple function was applied to describe the logical relationships of the factors and indices forming the vulnerability index. However, urban societies tend to respond to coastal hazards in a non-linear manner (Schiller et al., 2007). More sophisticated models considering non-linear causal relationships among different environmental factors and vulnerability indices are needed.

Given the importance of sustainable coastal development, appropriate adaptive responses should be incorporated into management plans to deal with the threats of natural hazards driven by climatic and human stresses. Synthetical vulnerability assessments are important for the implementation of national and location-specific interventions for mitigating adverse pressures. The assessment framework proposed in this study captures ecological, biophysical and socioeconomic factors and provides valuable information about the combined impacts of climate change (e.g., sea level rise), socioeconomic development and adaptation characteristics on coastal vulnerability. As datasets about the specific factors could be collected from the repositories of different administrative units (e.g., villages, provinces and countries), this study demonstrated the feasibility of providing decision-making supports by updating the maps and datasets available at different scales. The spatialization of CVIs benefits decision-makers by depicting highly-vulnerable areas as well as the critical factors affecting vulnerability, which are necessary analytical groundwork for developing efficient adaption strategies in the context of climate change.

5. Conclusions

The present study provided a holistic framework for synthetical vulnerability assessments by integrating ecological, physical and socioeconomic factors into a single spatial representation. The CVIs provided a macro-picture of the BER's heterogenous vulnerability at both segment and city scales under the current and future sea-level-rise scenarios. Currently, 20% of the coastlines with approximately 350,000 people are highly vulnerable to coastal hazards, and the number of highly-threatened population was estimated to increase by 13–24% with the rising sea-levels by 2100. Prioritized plans should be considered for the southwest and northeast coasts, and for the coast of Dongying, due to their higher risks compared to other cities. Several limitations of the framework proposed exist due to the oversimplification of the internal relationships among different environmental factors and vulnerability indices, and data deficiency on the dynamics of coastlines and natural habitats, as well as their community characteristics in the future. However, the framework is flexible and the results of this study can benefit decision-makers by highlighting coastal areas that should be prioritized for interventions by taking into account important influences that could be systematically evaluated at different scales, facilitating the

development of management plans to improve coastal adaptivity to climate change.

CRediT authorship contribution statement

Yan Zhang: Methodology, Data curation, Writing - original draft. **Tong Wu:** Writing - review & editing. **Katie K. Arkema:** Writing - review & editing. **Baolong Han:** Investigation. **Fei Lu:** Investigation. **Mary Ruckelshaus:** Writing - review & editing. **Zhiyun Ouyang:** Conceptualization, Supervision, Methodology.

Declaration of Competing Interest

The authors declare that they have no known competing financial interests or personal relationships that could have appeared to influence the work reported in this paper.

Acknowledgements

This work was supported by the National Natural Science Foundation of China (No. 71533005 and No. 41701549) and Youth Innovation Promotion Association, Chinese Academy of Sciences (No. 2013030).

Appendix A. Supplementary material

Supplementary data to this article can be found online at https://doi.org/10.1016/j.envint.2020.106359.

References

Arkema, K.K., Guannel, G., Verutes, G., Wood, S.A., Guerry, A., Ruckelshaus, M., Kareiva, P., Lacayo, M., Silver, J.M., 2013. Coastal habitats shield people and property from sea-level rise and storms. Nat. Clim. Change 3, 913–918.

Barbier, E.B., 2014. A global strategy for protecting vulnerable coastal populations. Science 345, 1250–1251.

Beroya-Eitner, M.A., 2016. Ecological vulnerability indicators. Ecol. Indic. 60, 329–334.

Bevacqua, A., Yu, D., Zhang, Y., 2018. Coastal vulnerability: Evolving concepts in understanding vulnerable people and places. Environ. Sci. Policy 82, 19–29.

Brooks, N., Adger, W.N., Kelly, P.M., 2005. The determinants of vulnerability and adaptive capacity at the national level and the implications for adaptation. Global Environ. Change 15, 151–163.

Chen, J., Ban, Y., Li, S., 2014. China: Open access to Earth land-cover map. Nature 514, 434.

Gabler, C.A., Osland, M.J., Grace, J.B., Stagg, C.L., Day, R.H., Hartley, S.B., Enwright, N. M., From, A.S., Mccoy, M.L., Mcleod, J.L., 2017. Erratum: Macroclimatic change expected to transform coastal wetland ecosystems this century. Nat. Clim. Change 7, 142–147.

Gao, X., Zhou, F., Chen, C., 2014. Pollution status of the Bohai Sea: An overview of the environmental quality assessment related trace metals. Environ. Int. 62, 12–30.

Gedan, K.B., Kirwan, M.L., Wolanski, E., Barbier, E.B., Silliman, B.R., 2011. The present and future role of coastal wetland vegetation in protecting shorelines: answering recent challenges to the paradigm. Clim. Change 106, 7–29.

GIMCP, 2018. Geographical Information Monitoring Cloud Platform: Socioeconomic and infrastructure conditions for Bohai Economic Rim. http://www.dsac.cn. Accessed: 13-08-2018.

Gornitz, V.M., 1990. Vulnerability of the east coast, USA to future sea level rise. J. Coast. Res. 9, 201–237.

Hahn, M.B., Riederer, A.M., Foster, S.O., 2009. The livelihood vulnerability index: A pragmatic approach to assessing risks from climate variability and change - A case study in Mozambique. Global Environ. Change 19, 74–88.

Hammar-Klose, E.S., Thieler, E.R., 2001. Coastal vulnerability to sea-level rise: a preliminary database for the U.S. Atlantic, Pacific, and Gulf of Mexico coasts. (U.S. Geological Survey Digital Data Series 68, 2001). https://pubs.er.usgs.gov/publication/ds68. Accessed: 11-04-2018.

Hansen, J., Sato, M., Hearty, P., Ruedy, R., Kelley, M., Masson-Delmotte, V., Russell, G., Tselioudis, G., Cao, J., Rignot, E., Velicogna, I., Tormey, B., Donovan, B., Kandiano, E., von Schuckmann, K., Kharecha, P., Legrande, A.N., Bauer, M., Lo, K. W., 2016. Ice melt, sea level rise and superstorms: evidence from paleoclimate data, climate modeling, and modern observations that 2 °C global warming could be dangerous. Atmos. Chem. Phys. 16, 3761–3812.

He, Q., Silliman, B.R., 2019. Climate change, human impacts, and coastal ecosystems in the anthropocene. Curr. Biol. 29, R1021.

Hinkel, J., Klein, R.J.T., 2009. Integrating knowledge to assess coastal vulnerability to sea-level rise: The development of the DIVA tool. Global Environ. Change 19, 384–395.

Hopper, T., Meixler, M.S., 2016. Modeling coastal vulnerability through space and time. PLoS One 11, e0163495.

IPCC, 2014. Intergovernmental Panel on Climate Change. Climate Change 2014: Impacts, Adaptation, and Vulnerability. Part A: Global and Sectoral Aspects. Contribution of Working Group II to the Fifth Assessment Report of the Intergovernmental Panel on Climate Change [Field, C.B., V.R. Barros, D.J. Dokken, K.J. Mach, M.D. Mastrandrea, T.E. Bilir, M. Chatterjee, K.L. Ebi, Y.O. Estrada, R.C. Genova, B. Girma, E.S. Kissel, A. N. Levy, S. MacCracken, P.R. Mastrandrea, L.L. White (Eds.)]. Cambridge University Press, Cambridge, United Kingdom and New York, NY, USA, pp. 1132.

Kantamaneni, K., Phillips, M., Thomas, T., Jenkins, R., 2018. Assessing coastal vulnerability: Development of a combined physical and economic index. Ocean Coast. Manage. 158, 164–175.

Krishnan, P., Ananthan, P.S., Purvaja, R., Joyson, J.J.J., Amali, J.I., Srinivasa, C.R., Anand, A., Mahendra, R.S., Sekar, I., Kareemulla, K., 2019. Framework for mapping the drivers of coastal vulnerability and spatial decision making for climate-change adaptation: A case study from Maharashtra, India. Ambio 48, 192–212.

Liu, X.H., Liu, L., Peng, Y., 2017. Ecological zoning for regional sustainable development using an integrated modeling approach in the Bohai Rim. China. Ecol. Model. 353, 158–166.

Lu, Q., Gao, Z., Zhao, Z., Ning, J., Bi, X., 2014. Dynamics of wetlands and their effects on carbon emissions in China coastal region – Case study in Bohai Economic Rim. Ocean Coast. Manage. 87, 61–67.

Mcowen, C., Weatherdon, L., Bochove, J., Sullivan, E., Blyth, S., Zockler, C., Stanwell-Smith, D., Kingston, N., Martin, C., Spalding, M., Fletcher, S., 2017. A global map of saltmarshes. Biodivers. Data J. 5, e11764.

MNR, 2020. Ministry of Natural Resources of the People's Republic of China. China Maritime Disaster Bulletin 2009-2019. http://www.mnr.gov.cn/. Accessed: 13-04-2020.

NBS, 2020. National Bureau of Statistics. China Statistical Yearbook 2020. http://www.stats.gov.cn/. Accessed: 2-12-2020.

NCP, 2018. Natural Capital Project: InVEST Version 3.5.0 Sample Datasets. http://data.naturalcapitalproject.org/invest-data. Accessed: 11-10-2018.

Oliveira, G.L.T., Murton, G., Rippa, A., Harlan, T., Yang, Y., 2020. China's belt and road initiative: views from the ground. Polit. Geogr. 82, 102225.

Onat, Y., Marchant, M., Francis, O.P., Kim, K., 2018. Coastal exposure of the Hawaiian Islands using GIS-based index modeling. Ocean Coast. Manage. 163, 113–129.

Phillips, M.R., Powell, V.A., Duck, R.W., 2009. Coastal regeneration at Llanelli, South Wales, UK: Lessons not learned. J. Coast. Res. 25, 1276–1280.

PSMSL, 2018. Permanent Service for Mean Sea Level: Long-Term Sea Level Change Information from Tide Gauges along the Coast of China. http://www.psmsl.org. Accessed: 15-09-2018.

Qu, Y., Jevrejeva, S., Jackson, L.P., Moore, J.C., 2019. Coastal sea level rise around the China seas. Global Planet. Change 172, 454–463.

Sahin, O., Mohamed, S., 2014. Coastal vulnerability to sea-level rise: a spatial-temporal assessment framework. Nat. Hazards 70, 395–414.

Sajjad, M., Li, Y., Tang, Z., Cao, L., Liu, X., 2018. Assessing hazard vulnerability, habitat conservation, and restoration for the enhancement of mainland China's coastal resilience. Earths Future 6, 326–338.

Schiller, A., Sherbinin, A.D., Hsieh, W.H., Pulsipher, A., 2007. The vulnerability of global cities to climate hazards. Environ. Urban. 19, 39–64.

Sekovskia, I., Newton, A., Dennison, W.C., 2012. Megacities in the coastal zone: Using a driver-pressure-state-impact-response framework to address complex environmental problems. Estuar. Coast. Shelf Sci. 96, 48–59.

Serafim, M.B., Siegle, E., Corsi, A.C., Bonetti, J., 2019. Coastal vulnerability to wave impacts using a multi-criteria index: Santa Catarina (Brazil). J. Environ. Manag. 230, 21–32.

Sharp, R., Tallis, H.T., Ricketts, T., Guerry, A.D., Wood, S.A., Chaplin-Kramer, R., Nelson, E., Ennaanay, D., Wolny, S., Olwero, N., Vigerstol, K., Pennington, D., Mendoza, G., Aukema, J., Foster, J., Forrest, J., Cameron, D., Arkema, K., Lonsdorf, E., Kennedy, C., Verutes, G., Kim, C.K., Guannel, G., Papenfus, M., Toft, J., Marsik, M., Bernhardt, J., Griffin, R., Glowinski, K., Chaumont, N., Perelman, A., Lacayo, M., Mandle, L., Hamel, P., Vogl, A.L., Rogers, L., Bierbower, W., D., D., Douglass, J., 2016. InVEST+ VERSION+User's Guide. The Natural Capital Project, Stanford University, University of Minnesota, The Nature Conservancy, and World Wildlife Fund. http://data.naturalcapitalproject.org/invest-releases/3.5.0/userguide. Accessed: 04-04-2018.

SOA, 2017. State Oceanic Administration. China Sea Level Bulletin 2017. http://www.mnr.gov.cn/sj/sjfw/hy/gbgg/zghpmgb. Accessed: 13-05-2018.

UNEP-WCMC, 2018. United Nations Environment-World Conservation Monitoring Centre: Global Distribution of Coastal and Oceanic Habitats. http://data.unep-wcmc.org/datasets. Accessed: 15-08-2018.

UNEP, 2006. United Nations Environment Programme. Marine and coastal ecosystems and human well-being: A synthesis report based on the findings of the Millennium Ecosystem Assessment. http://www.vliz.be/imisdocs/publications/120064.pdf. Accessed: 09-10-2018.

Wang, G., Liu, Y., Wang, H., Wang, X., 2014. A comprehensive risk analysis of coastal zones in China. Estuar. Coast. Shelf Sci. 140, 22–31.

Wang, Y., Mao, X., Jiang, W., 2018. Long-term hazard analysis of destructive storm surges using the ADCIRC- SWAN model: A case study of Bohai Sea, China. Int. J. Appl. Earth Obs. Geoinf. 73, 52–62.

Wei, F., Han, G.X., Han, M., Zhang, J.P., Li, Y.Z., Zhao, J.M., 2019. Temporal-spatial dynamic evoluation and mechanism of shoreline and the sea reclamation in the Bohai Rim during 1980–2017. Scientia Geographica Sinica 39, 997–1007.

Xu, L.L., Wang, X.M., Liu, J.H., He, Y.R., Tang, J.X., Nguyen, M., Cui, S.H., 2019. Identifying the trade-offs between climate change mitigation and adaptation in

urban land use planning: An empirical study in a coastal city. Environ. Int. 133, 105162.
Yadav, D.K., Barve, A., 2017. Analysis of socioeconomic vulnerability for cyclone-affected communities in coastal Odisha, India. Int. J. Disaster Risk Re. 22, 387–396.
Zhu, Z.T., Cai, F., Chen, S.L., Gu, D.Q., Feng, A.P., Cao, C., Qi, H.H., Lei, G., 2019. Coastal vulnerability to erosion using a multi-criteria index: a case study of the Xiamen coast. Sustainability 11, 93.